FATIGUE CHARACTERISTICS AND MICROSTRUCTURES OF LASER- AND NON-LASER WELDED LOW-COST Ti-4.5Al-2.5Cr-1.2Fe-0.1C FOR USE IN NEXT GENERATION AIRCRAFTS

Mitsuo Niinomi[1], Masaaki Nakai[1], Junko Hieda[1], Ken Cho[1], Yoshio Itsumi[2], Shogo Murakami[3], Hideto Oyama[2], Wataru Abe[4]

[1]Institute for Materials Research, Tohoku University, Sendai 980-8577, Japan
[2]Titanium Research and Development Section, Kobe Steel, Ltd., Takasago 676-8670, Japan
[3] Materials Research Laboratory, Kobe Steel, Ltd., Kobe 651-2271, Japan
[4]Material & Process Engineering Section, Aerospace Research Department, Engineering Division, Aero Space Co., Kawasaki Heavy Industry, Ltd., 1, Kawasaki-cho, Kagamigahara 504-8710, Japan

Keywords: Low-cost titanium alloy, KS-531C, Aircraft applications, Fatigue, Laser welding

Abstract

Ti-4.5Al-2.5Cr-1.2Fe-0.1C referred to as KS Ti-531C is a newly developed low cost titanium alloy for use in next-generation aircrafts by adding inexpensive elements such as C, Fe, Al and Cr. There is a possibility for the formation of TiCr and/or $TiCr_2$ after a long heat treatment or welding. Therefore, relationships between the microstructures and fatigue properties of KS Ti-531C subjected to several heat treatments as well as laser welding were investigated systematically. The results showed that the fatigue strength of laser-welded KS Ti-531C was lower than that of non-laser welded KS Ti-531C.

Introduction

Recently, a low-cost titanium alloy, Ti-4.5Al-2.5Cr-1.2Fe-0.1C (commonly referred to as KS Ti-531C) has been developed for use in next-generation aircrafts. This is achieved by adding inexpensive elements such as C, Fe, Al and Cr that impart the alloy good room-temperature mechanical properties (similar to those of Ti-6Al-4V ELI (Ti-64)), and high hot-workability with low flow stress during high-temperature deformation similar to that of commercially pure titanium (CPTi). Owing to these properties, KS Ti-531C can be used for fabricating forged and extruded components [1]. KS Ti-531C is obtained by modifying the chemical composition of the Ti-4.5Al-4Cr-0.5Fe-0.2C, also known as KS EL-F [2, 3]. The carbon content of KS Ti-531C is reduced to suppress titanium carbide precipitation; simultaneously, the chromium content is reduced and the iron content is increased to suppress $TiCr_2$ precipitation. However, the molybdenum equivalent of KS Ti-531C is almost identical to that of KS EL-F. Despite these processes, KS Ti-531C still contains a fairly large amount of carbon. The solid solubility limit of carbon decreases at temperatures near the β transus, in the range 1150–1300 K. This temperature range is often chosen for hot working and heat treatments to control the microstructures of (α + β)-type titanium alloys. Hence, there is a chance that titanium carbides might precipitate during the fabrication process of KS Ti-531C, and deteriorate mechanical properties of KS Ti-531C [1]. For aircraft materials, excellent fatigue strength and a good strength–ductility balance are essential. Herein the fatigue properties of KS Ti-531C, subjected to annealing at a temperatures

near the β transus, are described with a focus on the effects of high carbon content on these properties.

Titanium alloys used as aircraft materials are often utilized for fabricating components with complex shapes. In such cases, employing welded constructions is particularly effective for shortening the processing periods and reducing costs by decreasing the number of process steps [4]. Therefore, the improvement of welding techniques and the mechanical properties of welded components, fatigue strength, in particular, are much sought in the aerospace field.

Considering the dimensions and shapes of aircraft components, laser welding is preferred from the several welding techniques available. However, the microstructure of the laser-welded (α+β)-type titanium alloys is likely to be complex; it varies continuously from the welded zone to the matrix because melting and heating locally occur during welding. Therefore, the relationship between the microstructure and mechanical properties of laser-welded (α + β)-type titanium alloys should be understood more clearly. Further, studies on the effect of laser welding on the mechanical properties of KS Ti-531C, fatigue strength in particular have not yet been conducted.

In this paper, the microstructures and mechanical properties of KS T-531C, especially fatigue strength is also described.

Effect of Microstructure on Fatigue Strength of KS Ti-531C

The fatigue strengths of KS Ti-531C with two types of microstructure, namely ((α + β)-annealed and β-annealed) have been evaluated. Further the effect of carbide precipitation on their fatigue strength has been also investigated. The (α + β)-annealed and β-annealed KS Ti-531C exhibit an equiaxed and a Widmanstätten α structure respectively, as shown in Fig. 1 [5]. Their fatigue strengths are shown in Fig. 2 [5] as S–N (stress versus number of cycles) curves, along with the fatigue limit range of annealed Ti-64. The fatigue limit of (α + β)-annealed KS Ti-531C is around 830 MPa, which is higher than that of annealed Ti-64. The fatigue ratio defined as the value of fatigue limit divided by tensile strength of (α + β)-annealed KS-Ti-531C is 0.78, which is again higher than that of annealed Ti-64 that has a fatigue ratio in the range 0.42–0.62. The fatigue limit and fatigue ratio of β-annealed KS-Ti-531C are 675 MPa and 0.66, respectively, and are thus lower than those of (α + β)-annealed KS Ti-531C. However, the fatigue limit and fatigue ratio of β-annealed KS-Ti-531C are comparable to the upper limit of these corresponding values for annealed Ti-64.

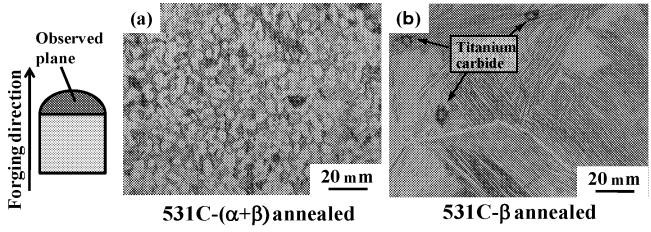

Fig. 1 Optical micrographs of cross-sections of (a) 531C-(α + β) annealed and (b) 531C-β annealed.

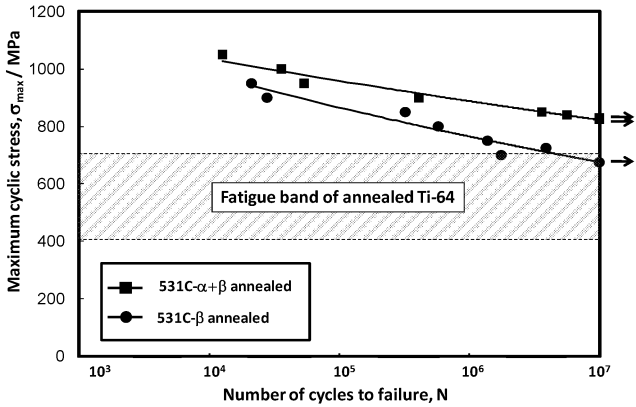

Fig. 2 Fatigue properties of 531C–(α + β) annealed and 531C-β annealed.

Figure 3 [5] shows the scanning electron microscopy (SEM) fractographs of (α + β)-annealed KS-Ti-531C after a fatigue test at number of cycles (N) > 10^5, for a high-cycle fatigue-life region. It can be seen that internal crack initiation occurs. Inclusions and pores are not observed, either at the crack initiation site or in the crack propagation area. A facet with morphology similar to a needle-like α-aggregate is observed at the crack initiation site, indicating that crack initiation occurs in a two-phase area (needle-like α + β) between primary α phases.

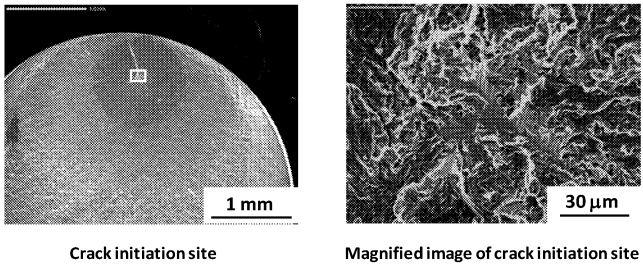

Fig. 3 SEM fractographs of 531C-(α + β) annealed after fatigue test in high-cycle fatigue life region ($N = 3.619 \times 10^6$).

Figure 4 [5] shows the SEM fractographs of β-annealed KS Ti-531C after a fatigue test at $N > 10^5$, for a high-cycle fatigue-life region. Internal crack initiation occurs as in the case of (α + β)-annealed KS Ti-531C. However, in this case, an inclusion is observed within a facet at the crack initiation site. Such an inclusion was not observed in the fatigue-fractured surface of (α + β)-annealed KS Ti-531C. Electron probe microanalyzer (EPMA) point analysis revealed that the chemical composition of this inclusion was found to be almost identical to that of titanium carbide, as shown in Fig. 4 [5]. Therefore, it can be concluded that titanium carbide induces crack initiation, leading to a deterioration in the fatigue properties of β-annealed KS Ti-531C compared to those of (α + β)-annealed KS Ti-531C.

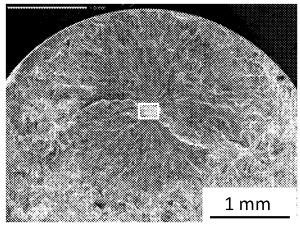

Crack initiation site

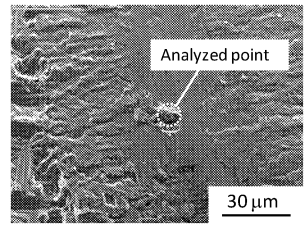

Magnified image of crack initiation site

Chemical composition (at.%)

Al	C	Fe	Cr	Ti
0.53	31.95	0.07	0.11	67.34

Fig. 4 SEM fractographs of 531C-β annealed after fatigue test in high-cycle fatigue life region ($N = 3.898 \times 10^6$) and result of EPMA point analysis of precipitate observed at crack initiation site.

Tensile Properties and Fatigue Strength of Laser Welded KS Ti-531C

Materials Preparation and Laser Welding [6]

After hot forging at 1373 K (in the β-phase region near the β transus temperature) and at 1173 K (in the (α+β)-phase region near the β transus temperature), an ingot of KS Ti-531C was hot rolled at 1173 K to a slab, and the thickness of the slab was reduced from 65 mm to 6 mm. The slab was annealed under vacuum at 978 K for 7.2 ks, followed by air cooling. Subsequently it was machined to a plate with a thickness of 5 mm. This sample is referred to as 531C-base.

Laser welding was carried out on 531C-base parallel to the transverse direction. Two types of welding conditions (A and B) were employed. Welding condition A involved welding from only one side of the plate surface. As shown in Fig. 5 (a) [6], laser was applied to the part where two plates were abutted. In one pass, melting occurred all the way from the surface to the back of the plates. On the other hand, welding condition B involved welding from both sides of the plate surface. As shown in Fig. 5 (b) [6], laser was first applied to the part where two plates were abutted, and the plates were welded to half of their thickness. Laser was then applied in the same manner to the abutting part from the back surface, and the plates were again welded to half of the thickness. Under the welding condition B, the depth to which melting was occurred in one pass was half of that in the case of welding condition A. The samples as-welded under welding conditions A and B are referred to as 531C-asweldA and 531C-asweldB, respectively. After welding under welding conditions A and B, the plates were annealed at 973 K for 7.2 ks, followed by air cooling. These samples are referred to as 531C-weldA and 531C-weldB, respectively.

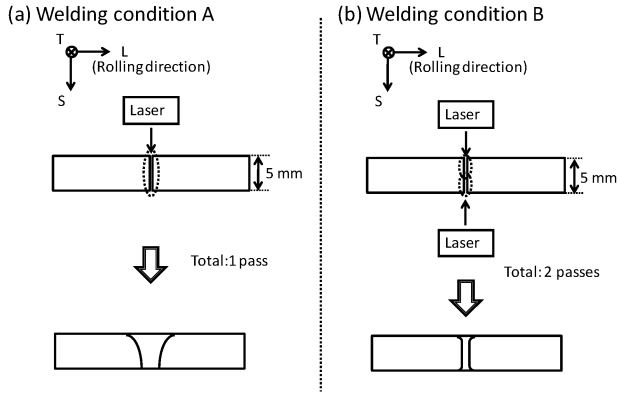

Fig. 5 Schematic drawings of laser welding conditions (a) A and (b) B employed in this study.

The longitudinal direction of the sample along the loading axis was set to be parallel to the L direction. The sample thickness was reduced to 3 mm by machining from both sides; the front and back of the samples on each L–T plane (rolling plane) were machined by 1 mm to make them 3 mm thick. The sample surface was then polished using SiC emery papers of up to #800.

Tensile Properties

Figure 6 [6] shows the tensile properties of 531C-base, 531C-weldA, and 531C-weldB. There is almost no difference between the tensile strengths of these materials. In this case, the longitudinal direction of the sample along the loading axis was set to be parallel to the L direction. The sample thickness was reduced to 3 mm by machining from both sides; the front and back of the samples on each L–T plane (rolling plane) were machined by 1 mm to make them 3 mm thick. The sample surface was then polished using SiC emery papers of up to #800.

Even in the case of 0.2% proof stress, no clear difference is observed among the three materials. Further these materials show nearly the same elongation values. In addition, the failure of 531C-weldA and 531C-weldB occurred in the matrix of the tensile sample, but no fractures occurred in the welded zone. On the basis of these results, it is clear that laser welding does not exert any negative effects on the tensile properties of Ti-531C. Accordingly, the tensile strength of KS Ti-531C in the L direction of the weld metal zone is higher than that of the matrix, and hence, failures occur in the matrix.

Fatigue Properties

Figure 7 [6] shows the fatigue properties of 531C-base, 531C-weldA, and 531C-weldB. In the figure, for comparison, the range of the fatigue limits for Ti64 subjected to laser welding [7] is also shown. The fatigue strengths of both welded samples are significantly lower than that of 531C-base. However, the fatigue strength of 531C-weldA is higher than the upper limit value of the fatigue strength of Ti64 subjected to laser welding, and thus a welded titanium alloy with relatively high fatigue strength is obtained. On the other hand, the fatigue strength of 531C-weldB is lower than that of 531C-weldA, and is slightly lower than the lower limit value of the fatigue strength of Ti64 subjected to laser welding. In addition, the failures of 531C-weldA and

531C-weldB occurred all in the welded zone of the fatigue specimens Figure 8 [6] shows the SEM fractographs of 531C-base, 531C-weldA, and 531C-weldB fractured in the high cyclic fatigue life region, observed after fatigue tests. For 531C-base, crack initiation was observed just under the surface of the specimens. At high magnification, flat facets in which inclusions were not particularly recognizable were observed at the crack initiation site of 531C-base. The facet shape is similar to the shape of the primary α phase in 531 C-base; it is considered that this similarity leads to crack initiation in the interior of the primary α phase in 531C-base or its grain boundaries. On the other hand, pores are observed at the crack initiation sites on the fractured surfaces of 531C-weldA and 531C-weldB. It should be noted here that no pores were observed on the fractured surfaces of 531C-base. The decrease in the fatigue strength of KS Ti-531C due to laser welding is predicted to be related strongly to the presence of these pores.

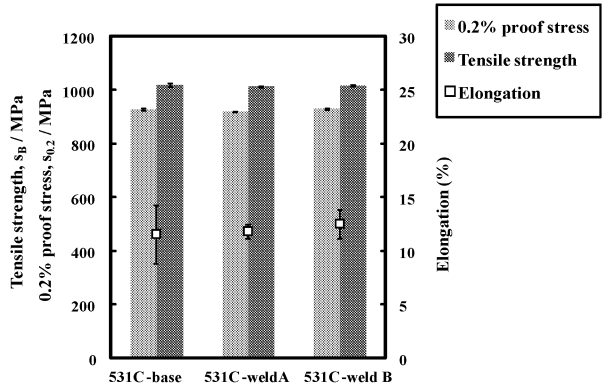

Fig. 6 Tensile properties of 531C base, 531C-weldA, and 531C-weldB.

Figure 9 [6] shows the relationship between the maximum stress intensity factor and the number of cycles to failure for 531C-weldA and 531C-weldB. When the fatigue properties of 531C-weldA and 531C-weldB are marshaled using the maximum stress intensity factor, the difference between them is reduced significantly in comparison to when they were evaluated using the maximum cycle stress (Fig. 9). Further, the values are found to be almost equal. This result indicates that the fatigue properties of welded samples depend largely on the diameters of pores or pore groups existing at the crack initiation site and that the effect of other microstructural factors on fatigue properties is small. The number of cycles to failure decreases with an increase in the maximum stress intensity factor. Moreover, the maximum stress intensity factor increases with an increase in the diameter of pores or pore groups. The average diameter of pores or pore groups in 531C-weldB is larger than that in 531C-weldA. Therefore, the fatigue strength of 531C-weldB is lower than that of 531C-weldA. As an overall trend, the fatigues strength of welded samples decreases with an increase in the diameter of pores or pore groups formed as weld defect during laser welding.

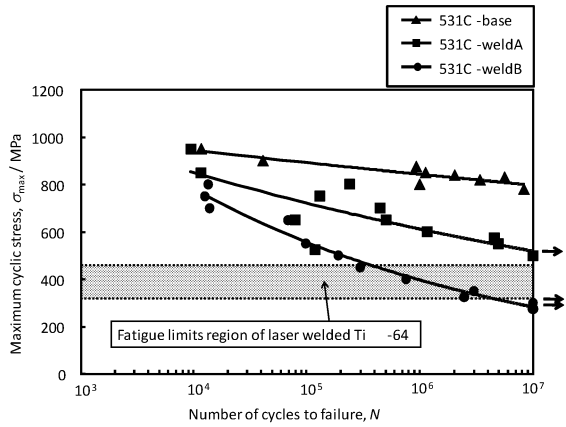

Fig. 7 Fatigue properties of 531C-base, 531C-weldA, and 531C-weldB.

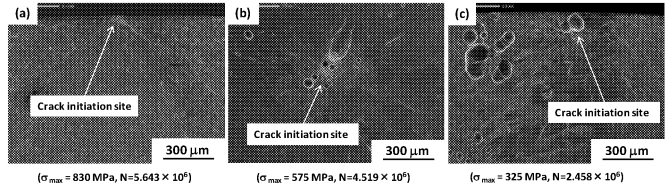

Fig. 8 SEM fractographs of (a) 531C-base, (b) 531C-weldA, and (c) 531C-weldB in high cyclic fatigue life region.

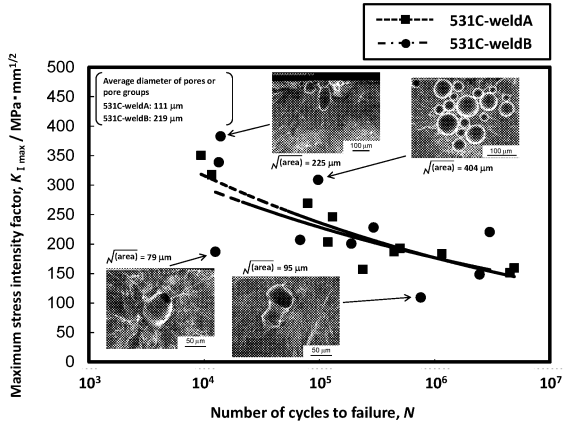

Fig. 9 Relationships between maximum stress intensity factor and number of cycles to fatigue failure of 531C-weldA and 531C-weldB.

Conclusions

1. The fatigue strength of β-annealed KS Ti-531C is lower than that of (α + β)-annealed KS-Ti-531C because of titanium carbide precipitation in the former. However, the fatigue strength of β-annealed KS Ti-531C is comparable to the upper limit of the fatigue strength of annealed Ti64.
2. The tensile properties of 531C-weldA and 531C-weldB exhibit a strength–ductility balance similar to that shown by 531C-base and no negative influence of laser welding on tensile strength is observed. All failures occurred in their matrix of these three samples because T-texture is formed in 531C-base, resulting in a decrease in hardness in the L direction.
3. The fatigue strengths of 531C-weldA and 531C-weldB are lower than that of 531C-base. Moreover, the decline in the fatigue strength of both welded samples is caused by the introduction of pores during welding. 531C-weldA, however, does posses improved properties in comparison to the laser-welded Ti-6Al-4V alloy that is a representative industrial titanium alloy.

Acknowledgements

This work was supported in part by the "Aerospace Industry Innovation Program—Advanced Materials & Process Development for Next-Generation Aircraft Structures" project under a contract with the RIMCOF Research Center of the Materials Process Technology Center, funded by the Ministry of Economy, Trade and Industry (METI) of Japan.

References

1. S. Murakami, K. Ozaki, K. Ono, and Y. Itsumi, in: M. Niinomi, S. Akiyama, M. Hagiwara, M. Ikeda, K. Maruyama (Eds.), *Ti-2007 Science and Technology,* The Japan Institute of Metals, Sendai, 2007, pp. 427-430.
2. H. Oyama, S. Kojima, K. Ono, and Y. Ito, *Mater. Sci. Forum*, 426-432 (2003) 713-718.
3. Y. Itsumi and H. Oyama, *R & D Kobe Steel Eng. Rep.*, 59(2009), 81-84.
4. R.R. Boyer, JOM 62 (2010) 21-24.
5. M. Nakai, M. Niinomi, J. Hieda, K. Cho, T. Akahori, K. Hayashi, Y. Itsumi, S. Murakamai, and H. Oyama, *Mater. Trans.*, 54(2013), 169-175.
6. M. Nakai, M. Niinomi, T. Akahori, K. Hayashi, Y. Itsumi, S. Murakami, H. Oyama, and W. Abe, *Mater. Sci. Eng. A*, 550(2012), 55-65.
7. R. Boyer, G. Welsch, and E.W. Collings, *Materials Properties Handbook: Titanium Alloys*, ASM International, Materials Park, OH, 1994.